J. Pharm. Pharmacol. 1997, 49: 403–411
Received September 10, 1996
Accepted January 3, 1997

A Comparison of the Physicochemical and Biological Properties of Mirtazapine and Mianserin

JAN KELDER, CAREL FUNKE, THIJS DE BOER, LEON DELBRESSINE, DIRK LEYSEN AND VICTOR NICKOLSON

NV Organon, Kloosterstraat 6, 5349 AB Oss, The Netherlands

Abstract

Although the chemical structures of the antidepressants mirtazapine and mianserin are closely related there are considerable differences in their biological properties. To find an explanation of this, various physicochemical properties of mirtazapine and mianserin were measured or calculated.

Isosteric replacement of CH in mianserin by N in mirtazapine has profound effects on physicochemical properties. The charge distributions as indicated by NMR and calculated by semi-empirical quantum mechanics differ, not only for the changed aromatic A-ring (as expected), but also in other regions of the molecule. The N5 atom in particular, which is conjugated to the changed aromatic ring, is less negatively charged in mirtazapine than in mianserin. Consequently the oxidation potential of mirtazapine is significantly higher than that of mianserin. Another result of this difference in charge distribution is that the (calculated) dipole-moment vectors of the compounds are oriented roughly perpendicular to each other. The dipole moment of mirtazapine is, moreover, three times larger than that of mianserin; mirtazapine is, therefore, more polar than mianserin and this is reflected in a lower retention index. Finally, the basicity of mirtazapine, expressed as the pK_a value, is slightly but significantly lower than that of mianserin.

The observed differences between the physicochemical properties of mirtazapine and mianserin result in different interactions of these two antidepressants with macromolecules, such as receptors, transporters and metabolizing enzymes; this might explain the differences observed in pharmacological activity and metabolic and kinetic behaviour, that is, the reduced affinity for the α_1-adrenoceptor and negligible noradrenaline re-uptake of mirtazapine compared with mianserin.

Minor changes in the chemical structures of therapeutically active molecules can result in remarkable changes in biological properties. This can be illustrated by the pharmacological and clinical differences between the structurally closely related antidepressants desipramine and imipramine, between imipramine and chlorimipramine, and between nortriptyline and amitriptyline (Hyttel 1982).

The chemical structure of the novel antidepressant mirtazapine is closely related to that of mianserin (Fig. 1). It was of interest to determine whether a seemingly simple isosteric replacement of a methine group (in mianserin) by a nitrogen (in mirtazapine) at position 6 also has effects on the biological properties of these antidepressants. Because such effects are likely to be a result of changes in physicochemical properties, the aim of this study was to investigate experimentally and by quantum mechanical calculation the physicochemical differences actually found and the extent to which these translate into differences in in-vitro and in-vivo pharmacological properties and metabolic and kinetic behaviour.

Materials and Methods

Physicochemical studies

Log P and basicity. Log P and basicity (pK_a) were measured (Table 1) by potentiometric titration at 25°C with 0·5 M KOH using a Sirius PCA 101 instrument (Sirius, UK) and calculated with standard software. Only the N2 atom was titrated. For log P data a sample (approximately 5 mg) was weighed accurately into a titration vial and dissolved in a mixture of 1-octanol (0·25 mL) and Milli-Q water (20 mL). For pK_a measurements a sample (approximately 5 mg) was weighed accurately into a titration vial and dissolved in an aqueous mixture (20 mL) of 0·15 M KCl and 47% m/m methanol.

Retention indices. Retention indices were measured by HPLC with a reversed-phase μC18 Bondapak column; aqueous methanol buffered with tetramethylammonium hydroxide phosphate at pH 7·4 was used as the mobile phase at 37°C, as described in the literature (Baker & Ma 1979). The retention index scale is based on the relative retention of a homologous series of C_3–C_{23} 2-ketoalkanes and is found to be fairly independent of the exact composition of the aqueous methanol mobile phase. By definition, acetone and 2-butanone have retention indices of 300 and 400, respectively. Amaranth was used as the t_0 marker. Measured retention indices (Table 1) are accurate to approximately 50 units.

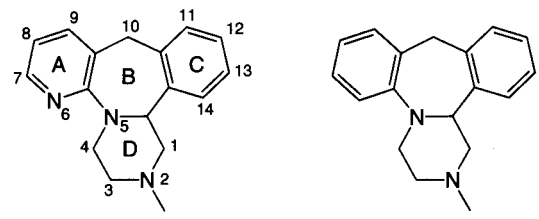

FIG. 1. Structures of mirtazapine and mianserin.

Correspondence: J. Kelder, NV Organon, Kloosterstraat 6, 5349 AB Oss, The Netherlands.

Table 1. Some experimental and calculated physicochemical data for mirtazapine and mianserin.

Property	Mirtazapine	Mianserin
Basicity (pK_a)	7·1	7·4
Partition coefficient (log P)	3·3	4·0
Retention index	910	1120
Experimental dipole moment (Debye)	2·63	0·82
Dipole moment (calculated [AM1]; Debye)	1·68	0·69
Dipole moment (calculated [PM3]; Debye)	1·77	0·55
Ionization potential (calculated [AM1]; eV)	8·77	8·52
Ionization potential (calculated [PM3]; eV)	8·78	8·69
Electrochemical oxidation potential (Volt)	+0·83	+0·76

Dipole moments. Dipole moments of the free bases of mianserin and mirtazapine were determined by measuring the dielectric constant ε of a series of diluted dioxane solutions at 25°C in a temperature-controlled sample holder using a precision bridge system of the WTW Kahlsico DM 01 dipole meter. The same solutions were used for measurement of the refractive indices (Abbe refractometer). Stock solutions (0·01 M; 100 mL) were diluted to four concentrations. The density, ρ, of dioxane at 25°C is 1·0267 g mL^{-1} and does not change dramatically at the highest concentration of 0·01 M (1·0270 g mL^{-1}). The Hedestrand equation (Hedestrand 1929) was used to calculate the molecular dipole moments of the compounds at extrapolated infinitely low concentrations. The results for mirtazapine and mianserin (Table 1) are accurate to 0·05 Debye.

Electrochemical oxidation potentials. Electrochemical oxidation potentials ($E_{p/2}$) of mirtazapine and mianserin were measured voltammetrically at a glassy carbon electrode (GCE) against a standard Ag/AgCl reference electrode. By applying a controlled potential over the electrode in an electrolysis cell, the electro-active compound can be oxidized and the oxidation potential ($E_{p/2}$) is measured at 50% of the maximum current. The compounds were dissolved (0·001 M) in a mixture of 0·005 M NaAc and HOAc and 0·1 M sodium perchlorate buffer in 90% methanol–water (apparent pH 6·8). Linear sweep voltammograms were run from −0·4 V to +1·6 V using Autolab (ECO-Chemie, The Netherlands) equipment connected with a VA 663 stand (Metrohm, Switzerland); the scan rate was 5 mV s^{-1}. Oxidation potentials ($E_{p/2}$) in Table 1 are accurate to 0·02 V.

Nuclear magnetic resonance (NMR) data. ^1H and ^{13}C NMR experiments were performed on 0·19 M solutions of mirtazapine and mianserin in $CDCl_3$ in 5-mm tubes, using TMS ($\delta = 0$ ppm) as internal standard. ^{15}N NMR measurements were of 0·75 M solutions in $CDCl_3$ in 10-mm tubes with ^{15}N-labelled methyl nitrate ($CH_3{}^{15}NO_3$; $\delta = 379{\cdot}6$ ppm) as internal standard. All NMR spectra were obtained on a Bruker AM360 spectrometer operating at a ^1H frequency of 360·13 MHz. Data collection and processing were performed with standard Bruker DISNMR software. The ^1H spectra were obtained using 7·7-μs $\pi/2$ pulses, a recycle time (AQ + delay) of 5 s and a spectral width of 8000 Hz sampled over 64 k points. Composite-pulse proton-decoupled (CPD) ^{13}C spectra were obtained using 11-μs $\pi/2$ pulses, a recycle time of 2·3 s and a spectral width of 25 000 Hz sampled over 64 k points. CPD ^{15}N spectra were obtained using 31-μs $\pi/2$ pulses, a recycle time of 1·4 s and a spectral width of 20 000 Hz sampled over 32 k points. Phase-sensitive NOESY (2-dimensional nuclear Overhauser effect) experiments were performed using the phase-sensitive absorption mode (TPPI) and a mixing time of 0·7 s. The data were collected using a 7·7-μs $\pi/2$ pulse, a sweep width of 2463 Hz and 2 k data points in the t_2 direction and 512 t_1 increments with 32 scans (t_1 increment)$^{-1}$. Before Fourier transformation the 2D data were multiplied by a 90°-shifted sine-bell squared function in both directions.

Semi-empirical quantum mechanics. Atomic charges, ionization potentials and dipole moments of mirtazapine and mianserin were calculated using AMPAC AM1 Version 2·10 (QCPE 506) (Dewar et al 1985). Electrostatic potential mappings were generated for mianserin and mirtazapine by use of the VSS program (QCPE 249) and displayed with Chem-X modelling software (Chemical Design, Oxon, UK). AMPAC AM1 calculations were performed with full optimization of the structures. The initial structural geometries were taken from experimental X-ray structures and optimized with the Chem-X molecular mechanics force field (the N5 atom had to be specified as an sp3-type nitrogen atom). For comparison the newer MOPAC PM3 method (Stewart 1989a, b) version 6·00 (QCPE 455) was used to calculate ionization potentials and dipole moments after full optimization of the same set of molecules (Table 1).

Neurochemical studies

Radioligand binding. Radioligand binding was performed by rapid filtration assays, details of which have been described previously (De Boer et al 1988). Receptor binding experiments were performed with various ligands and inhibition of specific ligand binding was measured by competition with increasing concentrations of the compounds. IC50 values were determined and pK_i values were calculated from these by use of the Cheng–Prusoff equation (Cheng & Prusoff 1973).

Monoamine re-uptake. Monoamine re-uptake was measured as described previously (De Boer et al 1988). Transport of radiolabelled noradrenaline or 5-HT into synaptosomes, obtained by homogenization and centrifugation of rat-brain regions, was measured by separating the radiolabelled monoamines taken up by rapid filtration. Inhibition of transport by

the compounds was measured in competition experiments similar to the binding experiments resulting in pK_i values as described above.

Interactions of compounds with peripheral receptors. These were studied by use of isolated organs; details have been described extensively (De Graaf et al 1983). The prejunctional α_2-adrenoceptor was studied by measuring the field-stimulated contractions of the rat vas deferens using azepexole as an agonist (De Boer et al 1988). The postjunctional α_1-adrenoceptor was measured using noradrenaline to contract the isolated vas deferens (De Graaf et al 1983). Concentration–effect curves were measured in the presence of different concentrations of the compounds studied and pA_2 values were estimated using Schild analysis.

In-vivo microdialysis studies. These were performed essentially according to a method described elsewhere (Santiago & Westerink 1990). A detailed description of the experiments has been published elsewhere (De Boer et al 1996). Male Wistar rats, approximately 250 g, were fitted with two microdialysis probes implanted in the left and right ventral hippocampus. The outlet of one of the probes was connected to the injector of an HPLC system, the inlet to a micro-infusion pump. The ventral hippocampus was perfused with Ringer's solution (containing 147 mM NaCl, 4 mM KCl and 3·4 mM $CaCl_2$ and 50 μM fluoxetine; the last compound was added to prevent released 5-HT from being taken up) at a speed of 1·5 $\mu L\ min^{-1}$. Every 15 min a 20-μL sample was injected automatically on to the column of the HPLC system. The DOPAC and 5-HT present in the perfusate were determined by use of Thermo-Separation Products HPLC equipment (P 4000 pump, As 1000 autosampler and PC 1000 software) connected to an Antec Leyden CU-04-AZ electrochemical detector with an Antec VT03 cell and fitted with a reversed-phase column (Supelcosil LC8DB, dimensions 25 × 0·46 cm). The buffer was a mixture of 0·05 M acetic acid and 0·05 M sodium acetate, both containing 100 mg L^{-1} EDTA and 150 mg L^{-1} heptane sulphonic acid. The mobile phase was acetic acid–methanol–acetate, 63 : 18 : 19 (% v/v) filtered and degassed. Groups of seven rats were treated with saline, mirtazapine (2 and 5 mg kg^{-1} s.c.) or mianserin (2 and 5 mg kg^{-1} s.c.). All data were expressed as percentage of the averaged baseline release in three consecutive samples collected immediately before injection of drug or saline. Areas under the curve from 0 to 150 min after injection were calculated for the various monoamines and used for treatment comparisons.

Kinetic and metabolism studies

Chemicals. 12-[^{3}H]-mirtazapine and 12-[^{3}H]-mianserin used for animal experiments and [10-^{14}C]-mirtazapine and 10-[^{14}C]-mianserin used for experiments with man were prepared by the Organic Synthetic Group, DMK Dept, NV Organon, Oss, The Netherlands. Radiochemical purity was > 98%. Reference compounds used for the identification of the urinary metabolites were synthesized by authentic routes. Chemicals of analytical quality were obtained from local commercial sources.

Drug administration and collection of excreta. Volunteers received radioactive [10-^{14}C]-drug as a mixture with lactose in snap-fit hard-shell gelatin capsules. Unlabelled and radioactive [12-^{3}H]-drug were administered to animals as an aqueous suspension in gelatin (0·5%) and mannitol (5%); dosing was by gastric intubation. Blood, urine and faeces were collected throughout the study. Samples of blood were centrifuged to prepare plasma. All samples were frozen at −20°C and stored deep-frozen until assayed.

Radiochemical techniques. Urine, urinary extracts, faeces extracts, column eluate, etc., were analysed by liquid scintillation counting. HPLC eluate was monitored for radioactivity by off-line liquid scintillation counting or by directly interfacing the HPLC with a flow-through radioactivity detector (Ramona, Isomess, FRG) coupled with a data system.

Chromatographic profiling and isolation of metabolites. Chromatographic profiles of the parent drug and its metabolites in the urine and faeces from the volunteers and from each group of animals were obtained by TLC autoradiography and by HPLC. Metabolites were isolated and purified either by repetitive preparative TLC in several solvent systems, by HPLC with several elution programs, or by a combination of both techniques, depending on the circumstances. Metabolites were tentatively identified by their TLC and HPLC properties (comparison with reference compounds). Confirmation of the identities of the metabolites was obtained by ^{1}H NMR spectrometry, mass spectrometry and occasionally by infrared spectroscopy.

Results

Physicochemical studies

Geometry. The molecular geometry of mirtazapine as determined by X-ray analysis (Van Meersche & Declercq, personal communication) is very similar to that of mianserin (Van Rij & Feil 1973; Van Meersche & Declercq 1983). The structures of the *S* enantiomers of both molecules are shown in Fig. 2. There is an anti relationship between the lone pair of the N5 atom and the adjacent 14b-hydrogen. The D-ring adopts a chair conformation with the *N*-methyl group in the energetically more favourable equatorial position. The N5 is a tetragonal rather than trigonal atom. The methylene C10 bridge of the B-ring is *anti* to the 14b-hydrogen in both molecules. The angle between the aromatic A and C rings is 115° for mirtazapine and 106° (Van Rij & Feil 1973) or 111° (Van Meersche & Declercq 1983) in both X-ray analyses for mianserin.

The ^{1}H, ^{13}C and ^{15}N chemical shifts of mirtazapine and mianserin are listed in Table 2. For mianserin the spectral data and their interpretation have been published (Funke 1982) and point to the same conformation in solution as depicted above for the crystalline state. Apart from the few differences discussed below, the chemical shifts of mirtazapine are quite similar to those of mianserin, which is indicative of the same conformation. This is further corroborated by the similar NOEs (nuclear Overhauser effects, Table 3). Strong mutual NOEs between the axial protons at positions 1 and 3, and at positions 4 and 14b, and between the axial proton at position 1 and the pseudoaxial proton at the C10 bridge are found for both compounds; these effects prove the chair-form of the piperazine ring and the out-of-plane position of the C10 bridge in the folded seven-membered ring (Fig. 2).

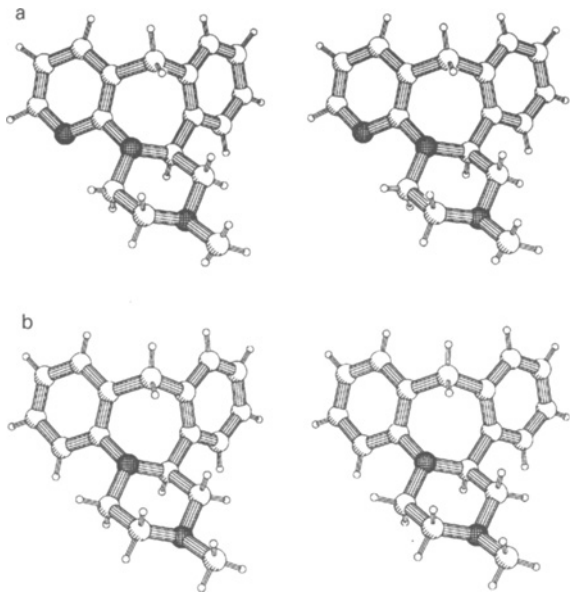

FIG. 2. The molecular geometry of mirtazapine (a) and mianserin (b) as determined by X-ray analysis.

Electron density. The main chemical shift differences between mirtazapine and mianserin are found for the protons, carbons and nitrogen at positions 4, 5, 14b and at the aromatic A-ring. These differences can be rationalized well in terms of the substitution of the mianserin benzene ring for a mirtazapine pyridine ring with greater electron-withdrawing properties. On the basis of the linear relationship between the chemical shifts of the aromatic carbons and the electron density at these carbons, the chemical shifts of C5a, C7 and (to a lesser extent) C9 are indicative of a lower electron density, whereas the shifts of C8 and C10a are indicative of a higher electron density at these atoms in mirtazapine than in mianserin. Similarly, the 13·4 ppm higher chemical shift of N5 suggests a lower electron density at this N-atom in mirtazapine than in mianserin.

The charge distributions calculated for mirtazapine and mianserin by use of the semi-empirical quantum mechanical method AMPAC with the AM1 Hamiltonian method are shown in Fig. 3. The N5 atom in mirtazapine is less negatively charged (−0·20) than the corresponding atom in mianserin (−0·26). There are no differences in the area of the basic N2 atom or in the C-ring. Most striking are the differences between the charge distributions in the A-ring. Fig. 4 shows contour plots of the electrostatic potential of the two molecules. The red-coloured contours show the positively charged areas; the cyan-blue areas are negatively charged. In mirtazapine the area near the pyridine nitrogen atom is negatively charged whereas in mianserin this area is weakly positively charged because of the presence of polarized C-H bonds. Fig. 4c shows the 3D contour plot of the difference between the electrostatic potentials of these two molecules superimposed on the structure of mirtazapine. This demonstrates clearly that the differences are most prominent around the C8–C10 part of the molecule and near the pyridine nitrogen atom. The less negatively charged N5 atom is also apparent. The experimental basicity data (pK_a; Table 1) also show a small but significant difference between mirtazapine and mianserin.

Dipole moment. Experimentally it was found that mirtazapine has a larger dipole moment than mianserin (Table 1). This was also calculated with the two semi-empirical methods described above (Table 1). The stronger dipole moment of mirtazapine leads to increased polarity and this is reflected in the lower retention index and lower log P values found experimentally (Table 1). The different charge distributions result in completely different orientations of the (calculated) dipole moments: the small dipole moment of mianserin,

Table 2. ^{1}H, ^{13}C and ^{15}N chemical shifts of mirtazapine and mianserin.

Atom	Mianserin			Mirtazapine		
	^{1}H*	^{13}C*	^{15}N†	^{1}H*	^{13}C*	^{15}N†
1	2·41/2·87**	64·97	–	2·51/2·85**	64·34	–
2	–	–	44·3	–	–	44·0
3	2·33/2·96**	55·59	–	2·33/2·96**	55·57	–
4	3·37/3·25**	51·28	–	3·48/3·70**	49·05	–
5	–	–	69·3	–	–	82·7
5a	–	148·70	–	–	159·40	–
6	–‡	119·06	–	–	–	288·5
7	7·16	126·98	–	8·15	146·26	–
8	6·86	122·28	–	6·72	117·06	–
9	–‡	129·55	–	7·31	134·56	–
9a	–	137·49	–	–	131·57	–
10	3·30/4·82**	38·83	–	3·41/4·52**	38·41	–
10a	–	139·83[a]	–	–	138·00[d]	–
11	–‡	128·14[b]	–	–§	129·69[e]	–
12	–‡	126·56[c]	–	–§	127·42	–
13	–‡	126·49[c]	–	–§	126·97	–
14	–‡	127·25[b]	–	–§	127·98[e]	–
14a	–	139·36[a]	–	–	137·07[d]	–
14b	4·07	66·58	–	4·35	64·80	–
15	2·36	45·85	–	2·36	45·85	–

*Referred to TMS ($\delta = 0$ ppm) as internal standard. †Referred to $CH_3\ ^{15}NO_3$ as internal standard ($\delta = 379{\cdot}6$ ppm). ‡Hidden in the overlapping aromatic multiplet at 6·98–7·14 ppm. §Hidden in the overlapping aromatic multiplet at 7·07–7·18 ppm. **Assigned in the order axial/equatorial (see text). [a,b,c,d,e]The assignment of these signals might be interchanged.

Table 3. Some ^{1}H–^{1}H NOEs as measured from the intensities of the cross peaks from NOESY experiments.

Proton	Mianserin			Mirtazapine		
	Strong	Medium	Weak	Strong	Medium	Weak
1ax	–	3ax, 10ax	–	–	3ax, 10ax	–
1eq	14*, 15	–	–	14*, 15	–	–
3ax	–	1ax	–	–	1ax	–
4ax	6*, 14b	–	–	14b	–	–
4eq	6*	–	–	–	–	–
10ax	–	1ax	–	–	1ax	9, 11*
10eq	9*, 11*	–	14b	9, 11*	–	14b
14b	4ax, 14*	–	10eq	4ax, 14*	–	10eq
15	1eq†	–	–	1eq, 1ax	–	–

*Based on tentative assignment. †NOE with H1ax not detectable because of signal overlap.

oriented almost parallel to the C1–C14b bond (Fig. 3b), differs by 104° from the direction of the much larger dipole moment of mirtazapine, which is oriented almost parallel to the C14a-C14b bond (Fig. 3a).

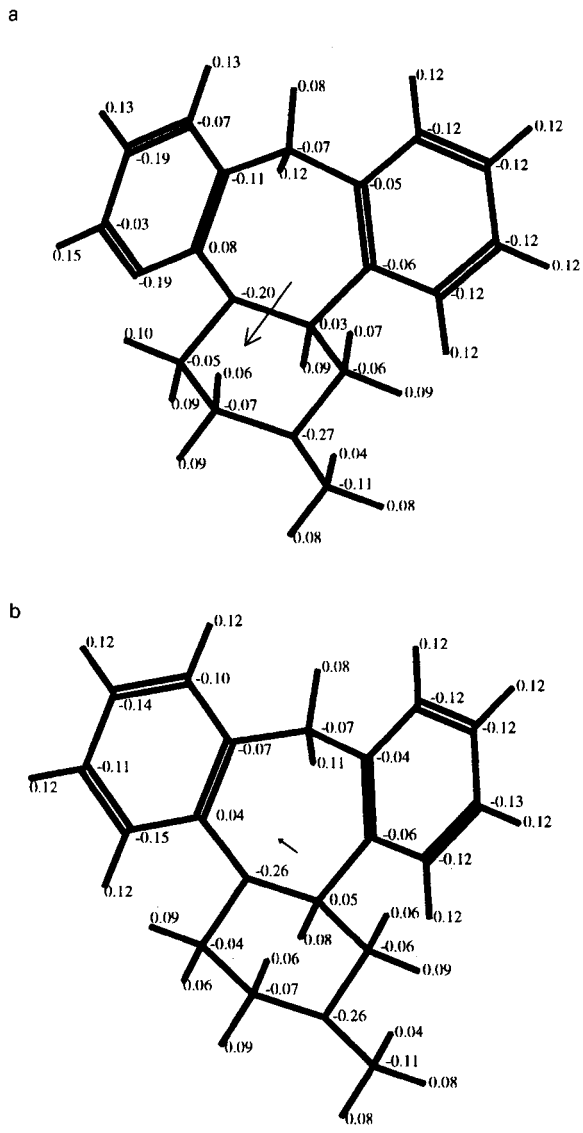

FIG. 3. AM1-calculated atomic charges in mirtazapine (a) and mianserin (b).

Oxidation potentials. The measured oxidation potentials of mirtazapine and mianserin are summarized in Table 1. The data show that the $E_{p/2}$ value of mirtazapine is higher than the corresponding value for mianserin; mirtazapine is oxidized less easily.

Neurochemical studies

Noradrenaline re-uptake (Table 4). Mianserin is a potent inhibitor of the re-uptake of noradrenaline, with a pK_i of 7·5. In contrast, mirtazapine has negligible effect on the re-uptake of noradrenaline ($pK_i = 5·8$; De Boer et al 1988).

Receptor binding (Table 4). In ^{3}H-rauwolscine-binding experiments both mirtazapine and mianserin have high affinity for central α_2-adrenoceptors; the pK_i values were 7·3 and 7·4, respectively. Mianserin also has high affinity for central α_1-adrenoceptors — pK_i value 7·1 in the ^{3}H-prazosin binding test. In contrast, mirtazapine has 10-fold lower affinity than mianserin for central α_1-receptors ($pK_i = 6·2$ in ^{3}H-prazosin binding; De Boer et al 1988).

Isolated organs (Table 4). Mianserin has threefold higher affinity than mirtazapine for peripheral α_2-adrenoceptors as measured in the stimulated isolated rat vas deferens preparation. In these experiments mianserin has a pA_2 value of 7·3 for antagonism of azepexole-induced contractions, whereas the pA_2 value for mirtazapine is 6·8. At peripheral α_1-adrenoceptors mianserin is a much stronger antagonist than mirtazapine. In the presence of cocaine to prevent interferences of compounds with the noradrenaline transporter, the pA_2 value of mianserin is 7·4, whereas mirtazapine ($pA_2 = 6·5$) is considerably less active.

Microdialysis studies. Mirtazapine (2 mg kg^{-1} s.c.) increases DOPAC levels in the perfusion fluid up to about 200% of baseline levels. The maximum level of DOPAC is reached in about 90 min and remains stable. Treatment with mianserin (2 mg kg^{-1} s.c.) causes a modest increase of DOPAC levels to about 30% above baseline (De Boer et al 1994, 1996).

Mirtazapine (2 mg kg^{-1} s.c.) rapidly increases 5-HT levels in rat hippocampus perfusates, reaching a maximum level of about 80% above baseline levels within 45 min after injection. Treatment with mianserin does not cause a statistically significant increase of 5-HT release. The effects of mirtazapine

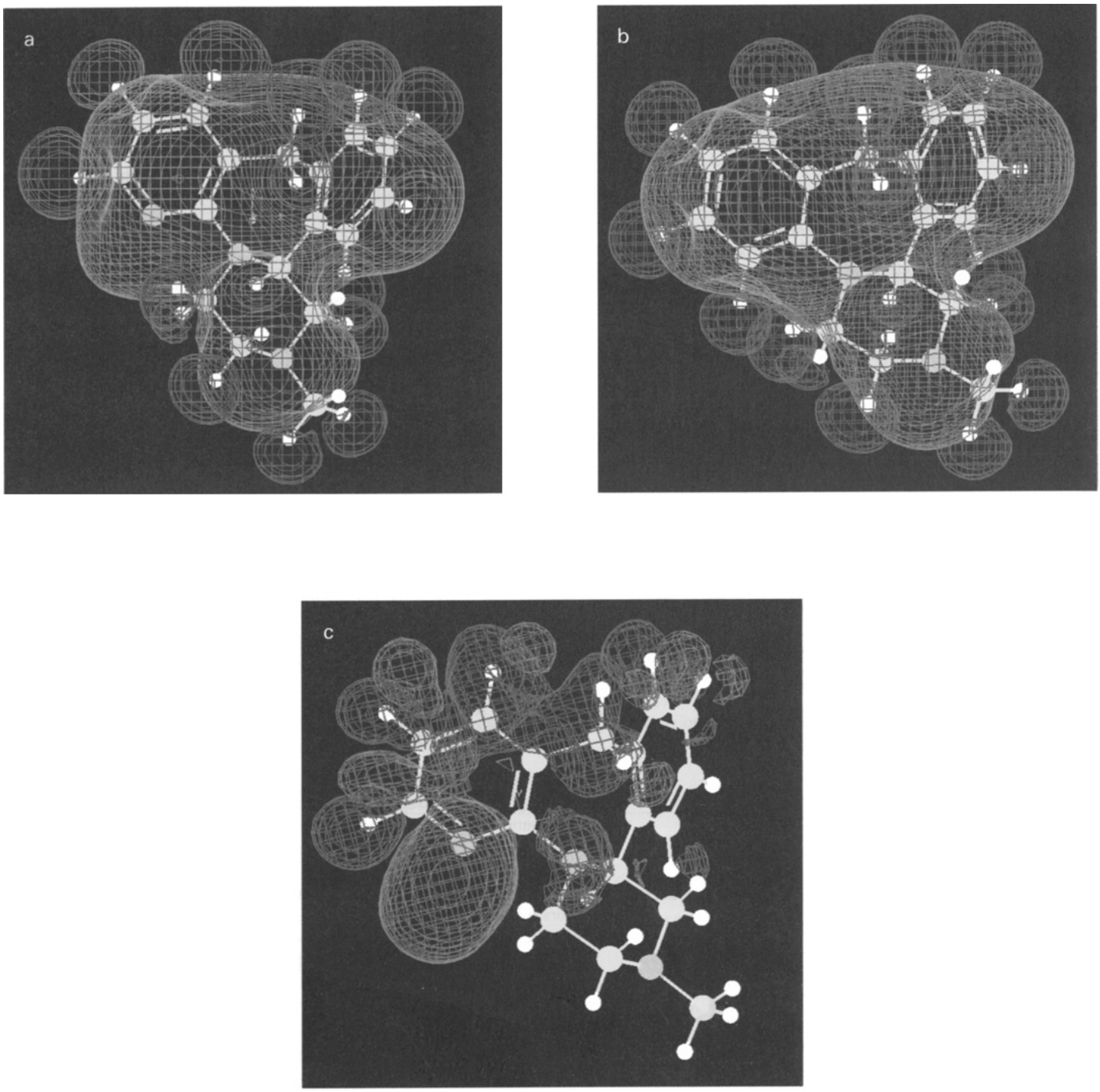

FIG. 4. Electrostatic potential energy contour plots of mirtazapine (a) and mianserin (b) displayed at −10 kcal mol^{-1} (cyan-blue) and +10 kcal mol^{-1} (red). The contour plot of the difference between the electrostatic potentials of mirtazapine and mianserin is also displayed on the structure of mirtazapine (c).

Table 4. Pharmacodynamic properties of mirtazapine and mianserin.

Receptor/transporter	Tissue	Parameter	Mianserin	Mirtazapine
Noradrenaline				
α_1-Adrenoceptor	Rat cortex	pK_i	7·1	6·2
α_1-Adrenoceptor	Rat vas deferens	pA_2	7·4	6·5
α_2-Adrenoceptor	Rat cortex	pK_i	7·4	7·3
α_2-Adrenoceptor	Rat vas deferens	pA_2	7·3	6·8
Noradrenaline				
Re-uptake	Hypothalamus	pK_i	7·5	5·8

and mianserin on DOPAC and 5-HT release have been compared on the basis of areas under the curve (De Boer et al 1994, 1996). The effects on DOPAC and 5-HT release are illustrated in Table 5.

Kinetic and metabolism studies

The metabolism of mirtazapine and mianserin is summarized and compared in Scheme 1.

Bioavailability and metabolism. Kinetic data for mirtazapine and mianserin show a difference in bioavailability. Mirtazapine has an absolute bioavailability of 50% in man (Voortman & Paanakker 1995) whereas that of mianserin is approximately 20% (Timmer et al 1985). On the basis of results from animal experiments and balance studies in man these differences in bioavailability cannot be explained by differences in absorption because both compounds are completely absorbed and extensively metabolized. The different absolute bioavailability differences might therefore be a result of differences in first pass metabolism.

The results of metabolism studies with labelled mirtazapine and mianserin in laboratory animals and human volunteers (De Jongh et al 1981; Delbressine et al 1992; Sandker et al 1994) demonstrate that both compounds are extensively metabolized and quantitatively eliminated via the urine and faeces within a few days and have several biotransformation routes in common: 8-hydroxylation then conjugation; N_2-demethylation then conjugation, N_2 oxidation and N_2 glucuronidation. The last pathway results in a metabolite that can be considered a prodrug; deconjugation of the glucuronic intermediate results in liberation of the parent compound. Investigative studies with ^{13}C-labelled and ^{12}C-mirtazapine showed that the formation of this intermediate occurred during passage through the wall of the intestine (Sperling et al 1994). Some remarkable differences in biotransformation pathways were found: mianserin underwent neither 13-hydroxylation then conjugation nor carbamate glucuronidation, as was found for mirtazapine, whereas mirtazapine did not undergo N-O glucuronidation, as had been found for mianserin.

Discussion

These experiments show that replacement of CH at position 6 in mianserin by N (in mirtazapine) results in profound changes in some physicochemical parameters. All experimentally detected and calculated differences between the physico-

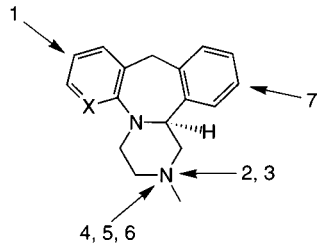

X = CH	X = CH or N	X = N
	1: 8-hydroxylation, then conjugation	
	2: N^+-glucuronidation	
	3: N-oxidation	
6: Demethylation, then oxidation and conjugation	4: Demethylation, then oxidation and conjugation	5: Demethylation, then CO_2-addition and conjugation
		7: 13-hydroxylation then conjugation

SCHEME 1. Metabolic pathways for mianserin and mirtazapine.

Table 5. The effects of mirtazapine and mianserin on noradrenergic and 5-HT-ergic transmission in the rat hippocampus.

	Increase in release (area under the curve)	
	DOPAC release	5-HT release
Control (saline)	10 ± 60	15 ± 110
Mirtazapine 2 mg kg^{-1}	630 ± 140**	530 ± 180**
Mirtazapine 5 mg kg^{-1}	740 ± 70**	520 ± 150**
Mianserin 2 mg kg^{-1}	200 ± 40*	240 ± 80
Mianserin 5 mg kg^{-1}	250 ± 60*	160 ± 70

The effect of subcutaneous administration of both compounds on the release of DOPAC and 5-HT was measured on the basis of AUC analysis of individual time-courses. *$P < 0.05$, **$P < 0.01$, significant compared with control (Student's t-test, $n = 7$).

chemical properties of the two molecules originate from the electron-withdrawing property of the pyridine ring in mirtazapine compared with the benzene ring in mianserin. Mirtazapine is a more polar compound and has a larger dipole moment that is oriented differently; it has different charge distribution in the A-ring resulting in a higher oxidation potential and lower basicity.

These considerable differences in dipole moment and basicity are expected to lead to differences in electrostatic interactions with macromolecules such as receptors, transporters and metabolizing enzymes. These results show that such differences exist: the affinities of mianserin for central and peripheral α_1-adrenoceptors and the central noradrenaline transporter are much higher than those of mirtazapine. This not only has consequences for central and peripheral noradrenergic processes but also for central 5-HT-ergic transmission. On the one hand, the α_2-receptor blockade-mediated increase of noradrenergic transmission (measured as DOPAC; De Boer & Ruigt 1995) in the brain appears to be lower after treatment with mianserin (increased noradrenaline levels as a result of reuptake blockade compete with mianserin for the presynaptic α_2-receptor) than after treatment with mirtazapine (no reuptake blockade). After treatment with mianserin, on the other hand, increased noradrenaline apparently fails to enhance 5-HT-ergic transmission because postsynaptic α_1-receptors mediating this effect are blocked by this drug (De Boer et al 1996). Because of the low affinity of mirtazapine for the α_1-receptor, the increased noradrenaline levels further enhance 5-HT-ergic transmission. On the basis of the potency difference at peripheral α_1-receptors it might be expected that mirtazapine causes less orthostatic hypotension than mianserin; data from the clinical studies suggest that this might indeed be true (Sitsen & Zivkov 1995).

The lower electron density in the A-ring of mirtazapine apparently leads to less 8-hydroxylation in this ring and this might explain why hydroxylation in the C-ring (at position 13) becomes a competing metabolic pathway for mirtazapine but not for mianserin.

Because of strongly reduced 8-hydroxylation, the competing biotransformation pathway in which direct conjugation at the N_2 position occurs is more pronounced for mirtazapine than for mianserin. This quaternary glucuronide, formed during passage through the intestine wall, is a prodrug of the parent compound; this might contribute to the twofold greater bioavailability of mirtazapine than mianserin.

The different biotransformation pathways for mirtazapine and mianserin do not account for the large difference in metabolic clearance. It might be suggested that lower lipophilicity, basicity and vulnerability to oxidation all contribute to the appreciably lower first-pass biotransformation of mirtazapine than of mianserin.

With regard to the potential for rare adverse drug reactions (Fisher et al 1991; Mason & Fisher 1992) it is postulated that under certain conditions desmethylmianserin can be transformed into the hydroxylamine intermediate, which further reacts to yield the isolated and identified N–O glucuronide. N_2 hydroxylation might be related to radical–cation formation, resulting in reactive intermediates. N_2 hydroxylation then glucuronidation has never been observed for mirtazapine. A plausible explanation might be that in contrast with desmethylmianserin, desmethylmirtazapine is in equilibrium with its CO_2 adduct from which the isolated and identified carbamate glucuronide is formed.

The different charge distributions in the A-ring result in a relative electron deficiency at N5 in mirtazapine. This suggests that electron abstraction at N5 should be more difficult in mirtazapine than in mianserin. It has been suggested that N5 in mianserin is involved in iminium ion (radical–cation) formation, leading to reactive metabolic intermediates (Roberts et al 1993).

Further studies are in progress to relate physicochemical differences between mirtazapine and mianserin to the propensity for radical formation and the differences in metabolic behaviour between mianserin and mirtazapine which are thought to be implicated in the occurrence of rare adverse drug reactions.

References

Baker, J. K., Ma, C.-Y. (1979) Retention index scale for liquid–liquid chromatography. J. Chromatogr. 169: 107–115

Cheng, Y. C., Prusoff, W. H. (1973) Relationship between the inhibition constant (K_i) and the concentration of the inhibitor which causes 50 per cent inhibition (IC50) of an enzymatic reaction. Biochem. Pharmacol. 22: 3099–3108

De Boer, T., Ruigt, G. S. F., (1995) The selective α_2-adrenoceptor antagonist mirtazapine (Org 3770) enhances noradrenergic and 5-HT_{1A}-mediated serotonergic neurotransmission. CNS Drugs 4 (Suppl. 1): 29–38

De Boer, T., Maura, G., Raiteri, M., de Vos, C. J., Wieringa, J., Pinder, R. M. (1988) Neurochemical and autonomic pharmacological profiles on the 6-aza-analogue of mianserin, Org 3770 and its enantiomers. Neuropharmacology 27: 399–408

De Boer, T., Nefkens, F., van Helvoirt, A. (1994) The α_2-adrenoceptor antagonist Org 3770 enhances serotonin transmission in vivo. Eur. J. Pharmacol. 253: R5–R6

De Boer, T., Nefkens, F., van Helvoirt, A., van Delft, A. M. L. (1996) Differences in modulation of noradrenergic and serotonergic transmission by the α_2-adrenoceptor antagonists mirtazapine, mianserin and idazoxan. J. Pharmacol. Exp. Ther. 277: 852–860

De Graaf, J. S., de Vos, C. J., Steenbergen, H. J. (1983) Fully automated experiments with isolated organs in vitro. J. Pharmacol. Toxicol. Meth. 10: 113–135

De Jongh, G. D., Van den Wildenbergh, H. M., Nieuwenhuyse, H., Van der Veen, F. (1981) The metabolism of mianserin in women, rabbits and rats. Drug Metab. Dispos. Biol. Fate Chem. 9: 48–53

Delbressine, L. P. C., Moonen, M. E. G., Kaspersen, F. M., Jacobs, P. L., Wagenaars, G. L. (1992) Biotransformation of mianserin in laboratory animals and man. Xenobiotica 22: 227–236

Dewar, M. J. S., Zoebisch, E. G., Healy, E. F., Stewart, J. (1985) AM1: a new general purpose quantum mechanical molecular model. J. Am. Chem. Soc. 107: 3902–3909

Fisher, V., Haar, J. A., Freiner, L., Lloyd, B. V. (1991) Possible role of free-radical formation in clozapine. Mol. Pharmacol. 40: 846–853

Funke, C. W. (1982) ^{1}H and ^{13}C spectra of mianserin and 10-hydroxymianserin derivatives in solution. Spectral assignments and conformational conclusions. Recl. Trav. Chim. Pays-Bas 101: 437–440

Hedestrand, G. (1929) Calculation of the molecular polarization of dissolved substances at infinite dilution. Z. Phys. Chem. (B) 2: 428–444

Hyttel, J. (1982) Citalopram: pharmacological profile of a specific serotonin uptake inhibitor with antidepressant activity. Prog. Neuropsychopharmacol. Biol. Psychiatry 6: 277–295

Mason, R. P., Fisher, V. (1992) Possible role of free radical formation in drug-induced agranulocytosis. Drug Safety 7 (Suppl. 1): 45–50

Roberts, P., Kitteringham, N. R., Parl, B. K. (1993) Elucidation of the structural requirements for the bioactivation of mianserin in-vitro. J. Pharm. Pharmacol. 45: 663–665

Sandker, G. W., Vos, R. M. E., Delbressine, L. P. C., Slooff, M. J. H., Meijer, D. K. F., Groothuis, G. M. M. (1994) Metabolism of three pharmacologically active drugs in isolated human and rat hepatocytes: analysis of interspecies variability and comparison with metabolism in vivo. Xenobiotica 24: 143–155

Santiago, M., Westerink, B. H. C. (1990) Characterization of the in vivo release of dopamine as recorded by different types of intracerebral microdialysis probes. Naunyn Schmiedebergs Arch. Pharmacol. 342: 407–414

Sitsen, J. M. A., Zivkov, M. (1995) Mirtazapine: clinical profile. CNS Drugs 4 (Suppl. 1): 39–48

Sperling, E., Delbressine, L., van Hal, H., Kaspersen, F. (1994) Pharmacokinetics and metabolism studies with ^{13}C-labelled mirtazapine. In: Allen, J., Voges, R. (eds) Synthesis and Applications of Isotopically Labelled Compounds. Wiley, pp 827–830

Stewart, J. J. P. (1989a) Optimization of parameters for semiempirical methods. I. Method. J. Comput. Chem. 10: 209–220

Stewart, J. J. P. (1989b) Optimization of parameters for semiempirical methods. II. Applications, J. Comput. Chem. 10: 221–264

Timmer, C. J., Pourbaix, S., Desager, J. P., Sclavons, M., Harvengt, C. (1985) Absolute bioavailability of mianserin tablets and solution in healthy humans. Drug Metab. Pharmacokin. 4: 315–323

Van Meersche, M., Declercq, J. P. (1983) Determination par diffraction de R-X de la structure de la mianserine. Bull. Soc. Chim. Belg. 92: 307–308

Van Rij, C., Feil, D. (1973) The molecular and crystal structure of (+)-mianserin hydrobromide. Tetrahedron 29: 1891–1893

Voortman, G., Paanakker, J. E. (1995) Bioavailability of mirtazapine from Remeron tablets after single and multiple oral dosing. Hum. Psychopharmacol. 10: S83–S96